Archives of Acoustics Vol. **47**, No. 2, pp. 201–212 (2022), doi: 10.24425/aoa.2022.141650

Research Paper

Objective and Subjective Assessment of the Sound Attenuation Efficiency Obtained by Custom Moulded Earplugs with Various Acoustic Filters – a Preliminary Study

Roman GOŁĘBIEWSKI, Andrzej WICHER*, Artur DURAJ,
Milena KACZMAREK-KLINOWSKA, Karina MRUGALSKA-HANDKE

Department of Acoustics, Faculty of Physics, Adam Mickiewicz University
Poznań, Poland
*Corresponding Author e-mail: awaku@amu.edu.pl

(*received June 27, 2021; accepted March 29, 2022*)

Background: Hearing loss caused by excessive exposure to noise is one of the most common health risks for employees. One solution for noise reduction is the use of hearing protectors, which is a very effective method for protecting hearing from the workplace noise. In order to obtain better attenuation efficiency, custom moulded earplugs can be equipped with a suitable acoustic filter. The effectiveness of the hearing protectors' attenuation is based on real measurement of hearing thresholds for normal hearing people with and without hearing protectors. However, this is a time consuming process, and the obtained values are characterised by quite large inter-individual variability. The optimal solution is to measure the attenuation characteristics based on the objective method (without the presence of the subject), the results of which will be in accordance with the results of subjective tests. Therefore, the main purpose of the research in this work was to measure the attenuation characteristics of the self-designed custom moulded earplugs with and without acoustic filters through the use of subjective and objective methods, and to compare the results in terms of the research methods.

Methods: Measurements of the acoustic attenuation obtained by custom moulded earplugs with designed F1, F2, and F3 acoustic filters (internal diameters d_{F1} = 1.25 mm, d_{F2} = 0.85 mm, and d_{F3} = 0.45 mm), as well as full insert earplugs (without any acoustic filters) were carried out using two methods: objective and subjective. The objective measurements were carried out in an anechoic chamber. The artificial head (High-frequency Head and Torso Simulator Brüel & Kjær Type 5128) was located at a distance of 3 m, directly opposite the loudspeaker. The test signal in the measurements was pink noise – in the frequency range up to 12.5 kHz and the level 85, 90, and 95 dB. The hearing protectors with and without acoustic filters were mounted in the Head and Torso Simulator which was connected with Pulse System Brüel & Kjær. Five normal hearing subjects participated in the subjective measurements. A pink noise signal was used for one-third octave bands: 125, 250, 500, 1000, 2000, 4000, and 8000 Hz. The attenuation value was defined as the difference (in dB) between the hearing threshold of the test signal with a hearing protector and the hearing threshold determined without a hearing protector.

Results: The results of the objective method proved that in addition to the significant impact of frequency on the attenuation values, the type of filter used in custom moulded earplugs also had a significant effect. In addition, the results of the objective method showed that in the whole frequency range the highest attenuation values are shown by the full earplugs, achieving slightly above 45 dB for frequency of 8 kHz. The attenuation values obtained from subjective measurements also confirmed that both the frequency and type of filter significantly affect the attenuation values of the tested hearing protectors.

Conclusions: The results of this study did not confirm the hypothesis that the measurement method had no significant effect on the attenuation characteristics of self-designed custom moulded earplugs with different types of acoustic filters. The largest differences in attenuation values between the type of measurement methods occur for the low frequency band (250 Hz) and for higher frequencies (4000 Hz mainly). The change of the internal diameter of the F1 filter from 1.25 mm to 0.85 mm (F2 filter) did not significantly affect the attenuation characteristics.

Keywords: hearing protector; earplug; acoustic filter; hearing loss; artificial head.

List of abbreviations

SNR – signal-to-noise ratio,
REAT – real ear attenuation at threshold,
ATF – acoustical test fixture,
ANOVA – analysis of variance,
FE – full earplug,
MIRE – microphone in real ear.

1. Background

Noise is defined as any unwanted sound which can be annoying or unsafe to human health, and which may increase the risk of an accident at work. Noise can cause sleep disturbance, worsening of speech intelligibility, as well as temporary or permanent hearing loss. Hearing loss is a process that usually develops over years, because it is usually painless, gradual, and practically imperceptible. The progress of hearing loss due to the chronic influence of noise depends on the level of noise exposure and its duration. Hearing loss caused by excessive noise levels is one of the most common health risks for employees. Over 20% of workers in Europe are at risk of permanent hearing loss (Lie *et al.*, 2016). According to Directive 2003/10/EC (2003), three levels of noise exposure limits are proposed, where the first (lower) limit for the equivalent daily noise exposure level is $L_{EX,8h}$ = 80 dB (Śliwińska-Kowalska, Zaborowski, 2017). This noise level is often exceeded: a comparable or higher noise level (instantaneous values) occurs, for example, along highways. Noise at the workplace can be limited by both organisational methods and technical means. Organisational methods include, for example, shortening the working time at workplaces where safe noise levels are exceeded, while technical means include, e.g., the use of noise barriers, etc.

In a situation where the above mentioned methods are ineffective or impossible to apply, the best solution that remains is the use of hearing protectors, which is one of the most effective methods for protecting hearing from noise at the workplace. There are many types of hearing protectors: earmuffs, earplugs, and custom moulded earplugs. Custom moulded earplugs are made on the basis of the ear impression. Such earplugs, after insertion, tightly close the external auditory canal. In order to obtain different attenuation efficiency, custom moulded earplugs can be equipped with a suitable acoustic filter. These are easily replaceable elements, which are selected depending on the acoustic conditions at the workplace. The selection of hearing protectors is carried out on the basis of measurements of sound pressure levels at the workplace. The choice of hearing protector means there is a need to determine the appropriate attenuation efficiency – this should not allow excessive acoustic protection. Such excessive protection could make it impossible to communicate with other people and hear warning sounds.

In the available literature, research topics concerning hearing protectors are mainly focused on the problem of how hearing protectors attenuate sounds with different frequency and time characteristics (broadband noise, bands of noise, sound pulses, gunfire) (Davis *et al.*, 2011; Biabani *et al.*, 2017; Fackler *et al.*, 2017; Samelli *et al.*, 2018). In addition, the effect of hearing protectors on the ability to determine the location of a sound source (Zimpfer, Sarafian, 2014; Brown *et al.*, 2015; Lee, Casali, 2017) also impacts the level of speech intelligibility (Bockstael *et al.*, 2011; Norin *et al.*, 2011; Brown *et al.*, 2015; Hiselius *et al.*, 2015; Lee, Casali, 2017), as well as more complex aspects of sound sensations, e.g., perception of the sound of musical instruments by musicians using hearing protectors are also examined (Killion, 2012). It turns out that in the case of musicians, the sound levels can reach very high values, in the order of over 100 dB, which, with long term exposure, may also result in hearing loss.

One of the problems resulting from the use of hearing protectors is the deterioration of speech intelligibility, especially when speech is presented against the background noise and when the level of speech sounds is low. Level dependent hearing protectors that enable the selection of signal enhancement depending on the sound level reaching the user are a partial solution here (Bockstael *et al.*, 2011; Brown *et al.*, 2015; Lee, Casali, 2017). However, in (Norin *et al.*, 2011), the authors showed that using 3 different passive hearing protectors did not determine the impact of the type of the protector on speech intelligibility against noise and showed that none of the hearing protectors significantly affected speech intelligibility. One significant factor influencing speech intelligibility was the signal-to-noise ratio (SNR).

In the case of level dependent hearing protectors (signal amplification function depending on the level of the input signal) a significant improvement in speech intelligibility was found, especially for lower SNR values (Hiselius *et al.*, 2015).

In the studies determining the effectiveness of the attenuation provided by hearing protectors, the key issue is the research methodology according to PN-EN-ISO 4869-1 (2018); its main advantage is real measurement of hearing thresholds for normal hearing people with and without hearing protectors. Comparison of hearing thresholds allows the attenuation provided by the earplug for the respective frequency bands to be determined. These attenuation values take into account all the subjective aspects of sound perception, but data collection is a time consuming process. It should be stressed that the obtained attenuation values are characterised by quite large inter-individual variability. However, this inter-individual variability allows the assumed protection value (APV) to be obtained, which is provided by the tested hearing protec-

tor and is determined for a specific part of the population.

Therefore, the optimal solution is to measure the attenuation characteristics based on the objective method (without the presence of the subject), the results of which will be in accordance with the results of the subjective tests. The best solution is to use an artificial head (head simulator) that contains full copy of the auricles and the ear canal. There are many models of artificial heads with artificial ears currently on the market, however, this equipment does not have a full copy of the ear canal.

One of the most important works on the comparison of research methods to determine the value of the acoustic attenuation of hearing protectors is (Berger, 2005). In this paper, the author compared three methods of measuring the effectiveness of hearing protectors, i.e., the real ear attenuation at threshold (REAT method standard, PN-EN-ISO 4869-1, 2018) and two objective methods: microphone in real ear (MIRE), consisting of placing the microphone inside, near the tympanic membrane, as well as the acoustical test fixtures – ATF, which uses artificial ear systems consisting of a microphone placed in a suitable cover connected with an acoustic coupler. The element of the artificial ear is connected to the amplifier system and the measuring system, which usually provides a comprehensive analysis of signals, mainly in terms of determining sound levels and assessing the spectral structure.

This work focuses on comparing the results obtained by the REAT and ATF methods. The objective method (AFT) used in the research is based on the latest B&K solution regarding the design solution of an artificial ear placed in an artificial head (Bruel & Kjaer type 5128-C). The latest version of the artificial ear has a full mapping of the external auditory canal, which guarantees attachment of the ear and earplugs analogous to the real ear and also allows for phenomena related to the occlusion effect and the influence of the residual volume of the ear canal on the transmission properties of acoustic energy. This technical solution is very important because the subject of the research in this work is individually fit hearing protectors, placed partly in the external ear canal, ensuring the system is tightly closed and the possibility of using passive acoustic filters.

Therefore, the main purpose of the research in this work was to measure the attenuation characteristics of the self-designed custom moulded earplugs with and without acoustic filters through the use of subjective and objective methods and to compare the results in terms of the research methods. It was assumed that the change of the inside diameter of the filters' openings every 0.4 mm would be large enough to obtain three significantly different frequency characteristics of sound attenuation, according to the principle that the smaller the diameter, the greater the sound attenuation, especially in the higher frequency range. Moreover, it was also assumed that the results of the objective and subjective studies would not show statistically significant differences. This will be the basis for further research and the development of objective and fast methods for determining the attenuation characteristics of custom moulded earplugs.

1.1. Noise assessment at workplace

The importance of using hearing protectors, including earplugs, is of particular importance at workplaces where noise levels may be significantly exceeded. In this section we quote the most important requirements and standards in terms of permissible noise levels in the work environment.

To assess noise at the workplace, the following quantities should be used, based on Regulation of the Minister of Labour and Social Policy of 6 June 2014, on the maximum permissible concentrations and intensities of agents that are hazardous for health at the workplace (Journal of Laws, 2014):

- $L_{\mathrm{EX,8h}}$ [dB] – daily noise exposure level,
- $L_{\mathrm{EX},w}$ [dB] – weekly noise exposure level.

The daily noise exposure level is defined as

$$L_{\mathrm{EX,8h}} = L_{\mathrm{Aeq},T_e} + 10\log\frac{T_e}{T_o}, \tag{1}$$

where L_{Aeq,T_e} is the time average sound level determined for the time of noise exposure, T_e, and T_o = 8 hours = 28800 s. T_e is the exposure time.

The weekly noise exposure is defined by the following equation:

$$L_{\mathrm{EX},w} = 10\log\left(\frac{1}{5}\sum_{i=1}^{n} 10^{0,1(L_{\mathrm{EX,8h}})_i}\right), \tag{2}$$

where the index i denotes the i-th day in a week, and $n = 5$ – denotes the number of working days during the week.

In addition, according to the above regulation (Regulation of the Minister of Labour and Social Policy of 6 June 2014 on Maximum Permissible Concentration and Intensity of Agents Harmful to Health in the Working Environment, Journal of Laws, 2014), for the purpose of determining acoustic conditions at the workplace, additional measures are used:

- $L_{\mathrm{C,peak}}$ [dB] – the C-weighted peak sound pressure level,
- $L_{\mathrm{A,max}}$ [dB] – the A-weighted maximum sound pressure level.

In order to determine the degree of noise exposure, the following legal acts should be used:

- PN-EN-ISO 9612 (2011), Acoustics – Determination of occupational noise exposure – Engineering method.

- PN-N-01307 (1994), Permissible noise values in the workplace. Measurement requirements.
- Regulation of the Minister of Labour and Social Policy of 6 June 2014 (Journal of Laws, 2014).

The methods of measuring the quantities characterising noise at workplaces have been presented in detail in (PN-N-01307, 1994). The standard also includes requirements for measuring the equipment along with the mode and frequency of measurements.

The standard presents two methods:

- the direct method, based on continuous measurement, during the time when the worker is exposed to noise, and on reading the values of determined quantities directly from meters, e.g. noise dosimeters or integrating sound level meters,
- the indirect method, which involves measuring noise in a time shorter than the one being evaluated and applying appropriate mathematical relationships to determine the required amounts.

The permissible values at the workplace are defined in Regulation of the Minister of Labour and Social Policy of 6 June 2014 (Journal of Laws 2014).

Table 1. Permissible values of noise at the workplace.

Noise descriptor	Permissible value [dB]
Daily noise exposure level during an 8-hour day, $L_{\mathrm{EX,8h}}$ and weekly noise exposure during a 5-day working week, $L_{\mathrm{EX},w}$ [dB]	85
The A-weighted maximum sound pressure level, $L_{\mathrm{A,max}}$ [dB]	115
The C-weighted peak sound pressure level, $L_{\mathrm{C,peak}}$ [dB]	135

According to Regulation of the Minister of Labour and Social Policy (Journal of Laws, 2014), in order to determine if there is no exceedance of the permissible noise level at the workplace, individual values may not exceed the values given in the table above. If at least one of these values is not retained then it is stated that the workplace exceeds the permissible noise level and appropriate noise minimisation measures should be taken.

When all the technical possibilities to reduce noise at the workplace are exhausted and one of the abovementioned values is still exceeded, the employer is obliged to provide the employees with hearing protection and inform them about the potential risk of hearing damage.

1.2. Custom moulded earplugs

One way of providing hearing protection at the workplace is through the use of custom moulded earplugs. Hearing protectors are earplugs made on the basis of impressions from the ears. They close the external auditory canal tightly and can be equipped with additional, easily exchangeable acoustic filters, characterised by different values of acoustic attenuation. The selection of these filters depends on the acoustic conditions – i.e., on the noise level at the workplace. It should be remembered that the selection of a hearing protector with a specific acoustic filter should ensure an adequate level of communication and that warning sounds are audible. The method for estimating the sound level when hearing protection is used is described in the PN-EN-ISO 4869-2 (2018). A well chosen hearing protector should ensure effective communication and hearing of warning sounds. A badly chosen hearing protector can lead to the effect of excessive protection. This effect is associated with too much noise suppression. This, in turn, may cause the employee to feel acoustic isolation from the surroundings and experience reduced communication possibilities as well as the lack of ability to hear alarm and warning sounds. As a result, this leads to work discomfort and may lead to the employee's rejection of the hearing protector.

The construction of an individual hearing protector with an acoustic filter is presented in Fig. 1. The acoustic filter is mounted in a special sleeve which is permanently glued to the insert/protector.

Fig. 1. Construction of an individual hearing protector (earplug). Left: the acoustic filter (red) is mounted in an acoustic tube (blue) which is permanently glued to the earplug. Right: an acoustic filter (white) and an acoustic tube (blue).

To determine the acoustic efficiency (suppression) of custom moulded earplugs, subjective and objective methods are used. The subjective method for measuring the acoustic efficiency of hearing protectors is provided by PN-EN-ISO-4869-3 (2007). This standard describes the subjective method of measuring the acoustic attenuation of hearing protectors at low sound pressure levels (close to the threshold of hearing). The method was developed to obtain attenuation values close to the maximum which are difficult to achieve in real conditions. The hearing threshold is measured with and without a hearing protector, similar to PN-EN-ISO-8253-2 (2010). The objective method for measuring protectors is given in PN-EN-ISO-4869-3 (2007). However, this standard applies to ear muffs.

2. Methods

2.1. Design of new acoustic filters

New acoustic filters were designed and manufactured for the purposes of this research. The cross-section of one of these filters is shown in Fig. 2. The filters were labelled with the symbols F1, F2, and F3.

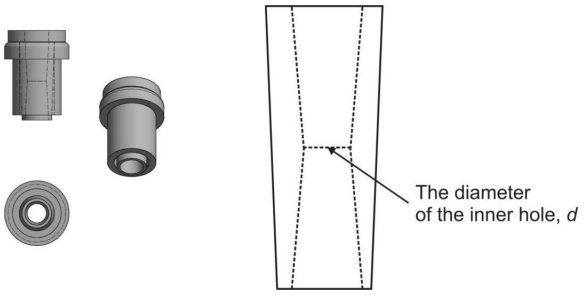

Fig. 2. Acoustic filter cross-section and longitudinal section.

The filters' openings are designed in the shape of a system of two cones with internal diameters d_{F1} = 1.25 mm, d_{F2} = 0.85 mm, and d_{F3} = 0.45 mm. Due to the quite typical shape of the filters (a system of two cones), it was assumed that the sound attenuation values would be higher in the higher frequency range. Moreover, it was also assumed that the change of the inside diameter of the filters' openings every 0.4 mm would be large enough to obtain three significantly different frequency characteristics, according to the principle that the smaller the diameter, the greater the sound attenuation, especially in the higher frequency range.

The filters' elements were designed using the Autodesk CAD Inventor software. The printing technique was applied with the help of the SLA FormLabs – form1 3D printer and the appropriate photosensitive resin. The process of preparing the filters consisted in measuring the geometry of the obtained filters and correcting the 3D model in order to eliminate the shrinkage of the resin which led to differences in the dimensions of the filters. The technique of stereolithography (SLA) was used, consisting in hardening the photosensitive resin with a laser beam. The printed out filters have been mechanically processed in order to get rid of unnecessary elements. Finally, the filters were exposed with UV rays in order to achieve the appropriate material hardness.

2.2. Determination of the acoustics attenuation obtained by custom moulded earplugs

Measurements of the acoustic attenuation obtained by self-designed custom moulded earplugs with designed F1, F2, and F3 acoustic filters, as well as full insert earplugs (without any acoustic filters) were carried out using two methods: objective (Subsec. 2.3) and subjective (Subsec. 2.4).

2.3. Objective method – measurements using a head simulator

The measurements were carried out in an anechoic chamber at the Institute of Acoustics of the Adam Mickiewicz University in Poznan.

The parameters of the anechoic chamber are presented in Table 2.

Table 2. Parameters of the anechoic chamber.

Parameter	Value
Dimensions (height/width/depth) [m]	6.5/6.5/8.5
Volume [m^3]	360
The lower frequency limit 80 [Hz]	80

The following measuring equipment was used in the measurements:

- High-frequency Head and Torso Simulator Brüel & Kjær Type 5128,
- Active Loudspeaker QSC type K10,
- System Pulse v. 12.6.0.255,
- Sound level meter Svantek type SVAN 945A.

The measurement system is presented in Fig. 3.

a)

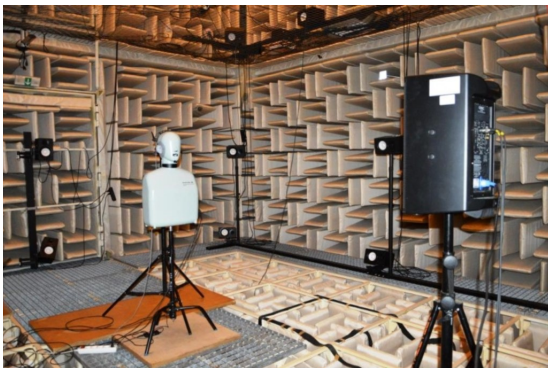

b)

Fig. 3. Artificial head with a torso made by the B&K company and a sound source placed opposite the dummy in an anechoic chamber. Front view (a) and side view (b) of the head and torso simulator.

It should be remembered that the Head and Torso Simulator Brüel & Kjær Type 5128 is characterised

by a complete mapping of the shape of the external ear canal, which is particularly important when testing earplugs. However, this equipment does not meet all the requirements of ANSI/ASA-S12.42-2010 (2010). In addition, this acoustic fixture test does not take into account the bone transmission (vibrations), which occurs with the perception of sounds in the auditory system. There is therefore some concern that, especially in the low frequency ranges, where bone conduction plays an important role, differences in acoustic attenuation values may arise with the objective and subjective methods.

The acoustic measurements were made for the following conditions:

- without hearing protectors,
- with hearing protectors without acoustic filters (the so-called full insert) and with acoustic filters mounted in the insert with the internal holes having different diameters, F1, F2, and F3.

The test signal in the measurements was pink noise – in the frequency range up to 12.5 kHz. The signal was generated by a loudspeaker (Active Loudspeaker QSC type K10). The artificial head (High frequency Head and Torso Simulator Brüel & Kjær Type 5128) was located at a distance of 3 m, directly opposite the loudspeaker. In addition, a sound level meter was located above the artificial head to calibrate the measuring system. The pink noise level was 85, 90, and 95 dB. The spectrum of the acoustic signal used in the tests is shown in Fig. 4.

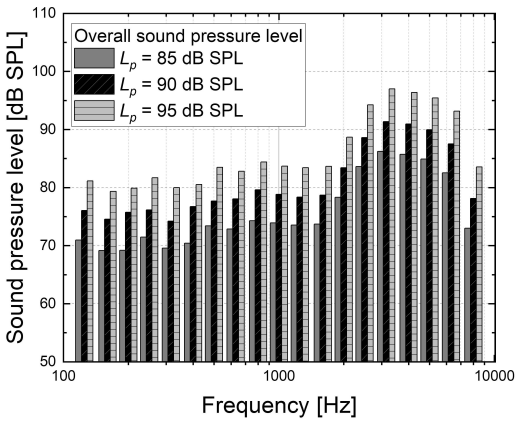

Fig. 4. One-third octave pink noise spectrum used in the study for three different total sound pressure levels (L_p = 85, 90, and 95 dB SPL).

2.4. Subjective method – measurements of the hearing thresholds

The subjective acoustic measurements were carried out in accordance with PN-EN-ISO 4869-1 (2018). Five students – students of the Institute of Acoustics (aged 20 to 22) participated in the measurements. According to the standard EN-ISO 4869-1 (2018), before starting the actual measurements, the subjects were checked for normal hearing. Hearing thresholds for participants should not exceed 15 dB HL in the 0.125–2 kHz band and 25 dB HL for frequencies above 2 kHz. The test for each listener was repeated at least 3 times for test signals, with the difference between the hearing thresholds for the middle frequencies not exceeding 6 dB. It should be emphasised that in the research the authors took into account a smaller number of subjects than is required by standard EN-ISO 4869-1 (2018). For this reason, each participant took part in the research three times. This approach was also related to the fact that this wass preliminary research and the authors took into account the number of participants in the next stages of the research. In Figs 5 and 6 there are the audiograms of people participating in the study.

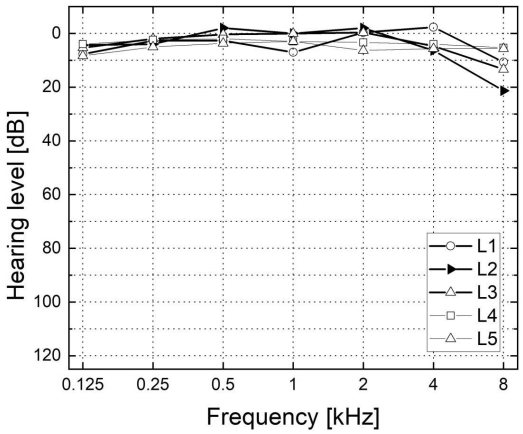

Fig. 5. Audiograms of subjects participating in the study (results for the right ear).

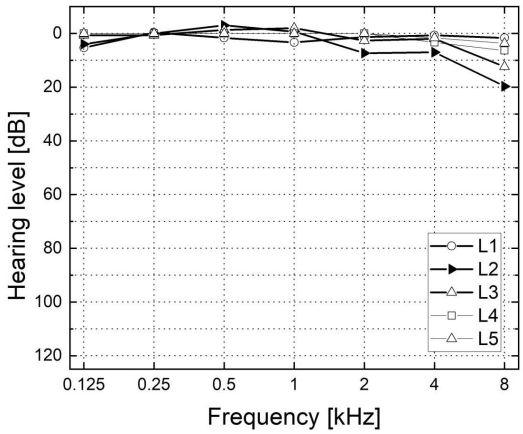

Fig. 6. Audiograms of subjects participating in the study (results for the left ear).

To determine the attenuation value obtained by the hearing protectors, a pink noise signal was used for one-third octave bands: 125, 250, 500, 1000, 2000, 4000, and 8000 Hz. The attenuation value was defined as the difference (in dB) between the hearing threshold of the test signal with a hearing protector and the hearing threshold determined without a hearing protector.

Measurements were made using an Interacoustics AC40 audiometer. As part of the work, measurements for each subject (for earplugs with different filters) were repeated three times. The level of background noise in the testing room did not exceed the permissible values for background sound pressure levels presented in the standard.

3. Results

3.1. Results of the objective method

As stated earlier, acoustic measurements were made for three scenarios: without earplugs, with full earplugs, and with earplugs with acoustic filters. During the acoustic measurements, the hearing protectors were located on both ears of the artificial head. The measurements were repeated five times for each condition. Before each subsequent measurement, the earplugs were removed and reinserted into the artificial ears.

The acoustic efficiency (attenuation) of hearing protectors with and without acoustic filters was determined as the difference between the sound levels recorded without earplugs and with earplugs – with different acoustic filters. Figure 7 shows the average values of attenuation as a function of frequency for individual earplugs equipped with F1, F2, and F3 filters and for the full earplug (FE). It can be unequivocally stated that in the whole frequency range the greatest attenuation is shown by the full earplug, achieving for 8 kHz average attenuation slightly above 45 dB. In the 0.5–2 kHz frequency band, the average attenuation increases by approx. 20 dB/octave, regardless of the earplug type. In turn, in the case of earplugs with filters, the maximum attenuation falls on the 2–4 kHz frequency band, and for 4–8 kHz decreases by about 6 dB.

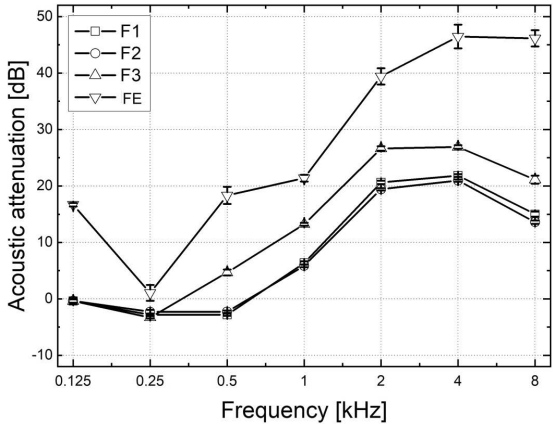

Fig. 7. Dependence of mean sound attenuation as a function of frequency, for the earplug with different filters (F1, F2, and F3) and for the full earplug (FE). Error bars show ±1 standard deviation.

3.1.1. Statistical analysis

In order to verify the research hypotheses regarding the influence of the acoustic filter diameter on changes in the earplug attenuation, an ANOVA analysis of variance was used. The dependent variable was the attenuation value of the earplug, while the factors were: "frequency", "filter type" and "pink noise level". The overall analysis showed that "frequency" is a factor significantly affecting the attenuation values $\{F(6) = 4720.91,\ p < 0.001\}$, similarly to "filter type" $\{F(3) = 4225.49,\ p < 0.001\}$. It was also verified whether the level of testing sound can affect the attenuation values obtained by the full earplugs and earplugs with acoustics filters.

The level of stimulation of the used pink noise turned out to be a factor that did not significantly affect the values of the attenuation of the earplugs with acoustic filters and in the case of the full earplug $\{F(2) = 0.841,\ p = 0.432\}$. The relationship between the attenuation values averaged over all the frequencies, for the individual filter type and for respective levels of stimulation is given in Fig. 8.

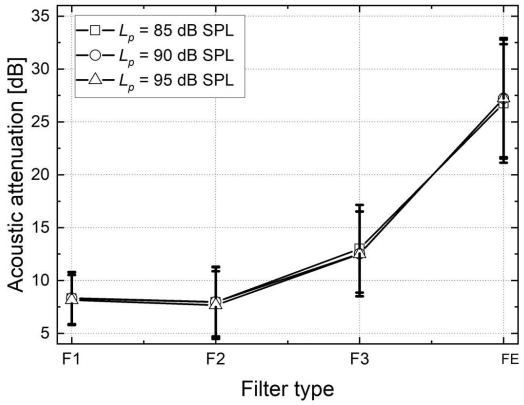

Fig. 8. Mean values of acoustic attenuation for the earplug with various acoustic filters (F1, F2, and F3) and for the full earplug (FE) as the function of levels stimulation. Error bars show ±1 standard deviation.

The Tukey test showed that at the confidence level $p = 0.05$, the average values of attenuation for earplugs with filters and full earplugs (FE) differ significantly. Analysis of the results by groups, according to the types of earplugs (with filters or full earplug) showed that for filters F1 and F2 the averaged attenuations do not differ statistically and are constant in the frequency band of 250–500 Hz (Fig. 7), while for each of the other frequencies the values of the average attenuations are different and these differences are statistically significant.

3.2. Results of the subjective method

The obtained values of acoustic attenuation for individual subjects and the average attenuation values

for the full earplugs with F1–F3 filters are shown in Figs 9–12.

Figure 13 shows a comparison of the mean attenuation for individual earplugs with acoustic filters and for the full earplugs. Figure 14 shows the attenuation values averaged over all the frequencies for individual earplugs with F1, F2, F3 filters and for the full earplugs.

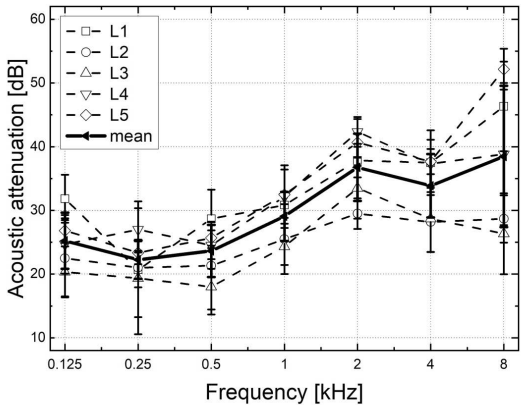

Fig. 9. Attenuation values for full earplugs (FE). The results are for individual subjects and average values, obtained using the subjective method. Error bars show ±1 standard deviation.

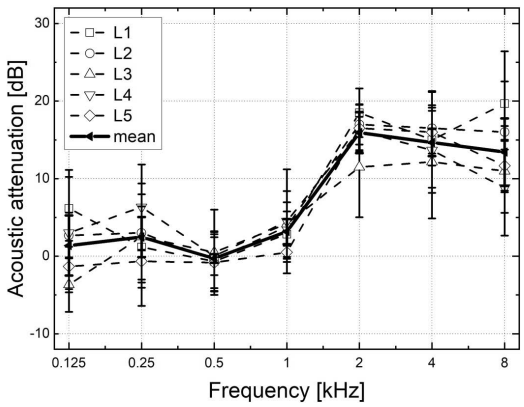

Fig. 10. Attenuation values for earplugs with acoustic filter F1. The results are for individual subjects and average values, obtained using the subjective method. Error bars show ±1 standard deviation.

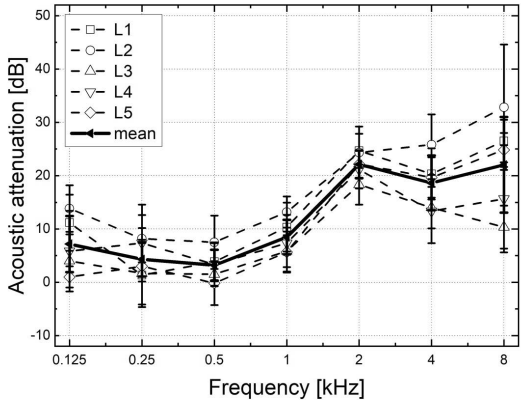

Fig. 11. Attenuation values for earplugs with acoustic filter F2. The results are for individual subjects and average values, obtained using the subjective method. Error bars show ±1 standard deviation.

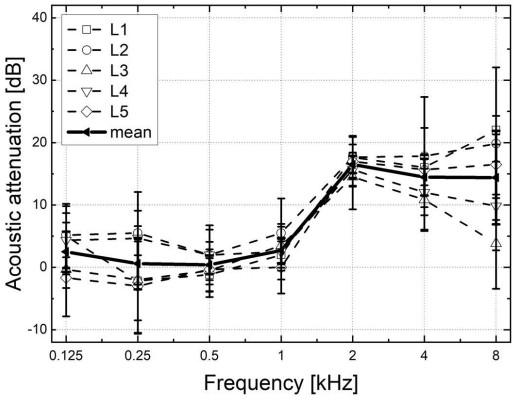

Fig. 12. Attenuation values for earplug with acoustic filter F3. Results for individual subjects and average values. Results obtained using the subjective method. Error bars show ±1 standard deviation.

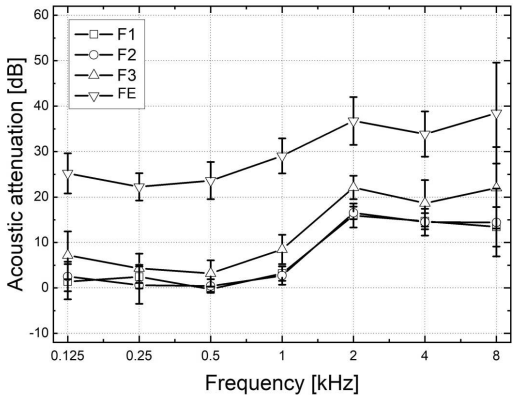

Fig. 13. Mean values of attenuation as a function of frequency for earplugs with F1, F2 and F3 filter and for full earplugs. The results are obtained using the subjective method. Error bars show ±1 standard deviation.

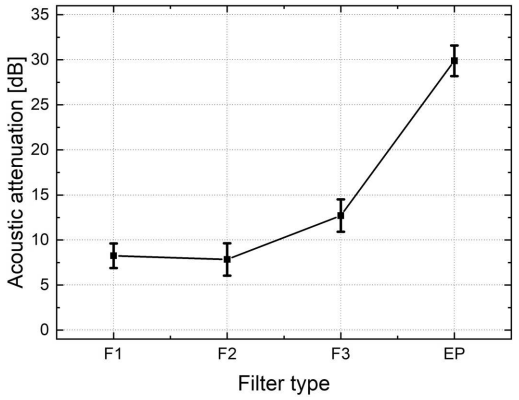

Fig. 14. Attenuation values averaged over all the frequencies for individual earplugs with acoustic filters (F1, F2, and F3) and for the full earplugs (FE). The results obtained using the subjective method. Error bars show 95% confidence interval.

3.2.1. Statistical analysis

The results obtained from the subjective method were also analysed on the basis of an ANOVA method in which the dependent variable was "attenuation", and the factors were: "frequency", "filter type". The main analysis of variance showed that both factors were statistically significant, at the significance level $p \leq 0.001$. This means that both "frequency" $\{F(6) = 111.41,\ p = 0.001\}$ and "filter type" $\{F(3) = 427.77,\ p = 0.001\}$ significantly affect the attenuation values of the tested earplugs. Tukey's test showed that at the confidence level of $p = 0.05$, the attenuation values for earplugs with F1 and F2 filters do not differ from each other, while there are significant differences in the attenuation values for the other cases, i.e., for the F3 filter and for full earplugs (EP).

This means that for all types of earplugs with filters and the full earplugs, the value of attenuation changed as a function of frequency. However, the average values of attenuation between F1 and F2 were not statistically significant. It can therefore be concluded that the attenuation characteristics of the earplugs with the F1 and F2 filters are comparable (Fig. 13). Only the use of the F3 filter or full earplug significantly changed the attenuation characteristics. This means that changing the inside diameter of the filter from 1.25 mm to 0.85 mm does not significantly affect the attenuation characteristics. Therefore, to attain greater diversity in the attenuation characteristics of the earplugs with filters, a filter with a diameter smaller than the F1 and F2 filters and larger than the F3 filter should be used. In addition, a filter with a smaller diameter than F3 should be used to obtain higher attenuation values, especially in the higher frequency band.

When analysing the results by group, according to the types of filters, it turned out that for earplugs with the F1 and F2 filters, the average attenuation values increase with increasing the frequency and differ significantly for the 0.125, 1, 2, 4, and 8 kHz frequency bands. It is only in the 0.25–0.5 kHz bandwidth that the attenuation values of the F1 and F2 filters do not show significant statistical differences. A similar relationship of attenuation values as a function of frequency was observed for the F3 filter.

The largest differences of the frequency response attenuation in relation to the F1, F2, and F3 filters are shown by the full earplugs (EP), i.e., it shows less selectivity of attenuation in individual frequency bands. The highest attenuation value falls within the 2–8 kHz frequency range and is approximately 36 dB, while in the 0.125–1 kHz range the attenuation value is smaller and amounts to approximately 24 dB.

The above analysis shows that the earplug combined with a properly selected acoustic filter allows to obtain a large diversity of attenuation values in each of the analysed frequency bands, which cannot be obtained with a full earplug.

3.3. Comparison of the results obtained by the objective and subjective methods

The next stage of the statistical analysis consisted in comparing the obtained results of acoustic attenuation for full earplugs and earplugs with different filters (F1–F3), as obtained by the subjective method and the objective method. Statistical analysis showed that for objective measurements the effect of the level of pink noise stimulation was not statistically significant, therefore this factor was not taken into account in these analyses. The factors were: "method", "frequency", and "filter type". A general analysis of ANOVA variance showed that "frequency" and "filter type" are the factors that significantly affect the sound attenuation obtained by earplugs $\{F(6) = 757.49,\ p < 0.001\}$ and $\{F(3) = 1340.46,\ p < 0.001\}$. It was shown that the "method" turned out to be statistically insignificant $\{F(1) = 0.36,\ p = 0.547\}$. However, this result is very generalised as it compares the average attenuation values obtained by the earplugs over all frequencies and over all types of earplugs. Tukey's post hoc analysis showed that for individual frequencies, the average sound attenuation values (taking into account all types of earplugs) differ significantly for the frequencies of 0.25 kHz and 4 kHz. As it is shown in Fig. 15, this figure presents the average attenuation values over all types of earplugs as a function of frequency for the objective and subjective methods.

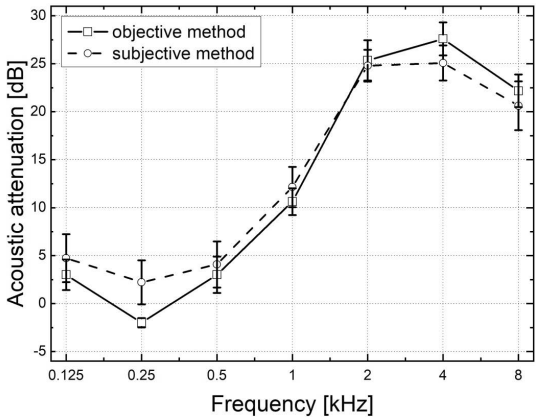

Fig. 15. Mean values of attenuation depending on the frequency obtained with the objective method (squares) and the subjective method (circles). Error bars show a 95% confidence interval.

As stated previously, the largest differences in attenuation values between the type of measurement methods occur for the low frequency band (250 Hz) and for higher frequencies (4000 Hz mainly). Most likely, this is related to the transmission of acoustic energy through vibrations of the skull/artificial head bones. In the low frequency band, bone conduction plays an important role in stimulating the inner ear and can be a significant factor in lowering the hearing

threshold in this frequency band. However, for high frequencies the attenuation of airborne sound in an artificial head may be less than that of a real ear.

4. Discussion

The research results presented in the paper showed that the average values of sound attenuation obtained by the applied self-design custom moulded earplugs, obtained on the basis of the objective and subjective measurement method, give comparable values (compare Fig. 8 with Fig. 14). However, when comparing the sound attenuation values obtained by the custom moulded earplugs for individual frequencies (Fig. 15), there appear to be already significant differences for the frequencies of 0.25 kHz and 4 kHz. It was particularly important that the change of the internal diameter of the F1 filter from 1.25 mm to 0.85 mm (F2 filter) did not significantly affect the attenuation characteristics.

Berger (2005) is one of the works with research topics very similar to the issues discussed in this article. The author compared three methods of measuring the effectiveness of hearing protectors, i.e., the real ear attenuation at threshold (REAT) method based on measuring the hearing threshold of people with hearing protectors and two objective methods. The first objective method is analogous to that used in this work, based on a measuring system consisting of an artificial ear/artificial head (acoustical test fixtures – ATF). The second objective method was to measure the sound level in the ear canal after putting on the hearing protector by placing a microphone near the eardrum (microphone in real ear-MIRE). In Berger (2005), the ATF method used an artificial head Brüel & Kjær Type 5128 which did not imitate the ear canal, while the artificial head used in the present work – Brüel & Kjær 5158 – used a full mapping of the ear canal. Berger (2005) obtained greater variances in the determined attenuation values, reaching about 20 dB for frequencies 4 and 8 kHz. In the conclusion of the work (Berger, 2005), it was stated that the REAT method is considered optimal, although it is not without drawbacks, such as those resulting from the need to involve a group of people to perform time consuming measurements. When the MIRE method is used, bone conduction is not included in the process of acoustic energy transmission. The optimal solution would be to use the ATF method to measure the attenuation characteristics of hearing protectors, both over-the-ear and in-the-ear, and this has been attempted in this study.

The work Kozłowski and Młyński (2017) focused on determining the attenuation characteristics of hearing protectors in the band above 8 kHz, i.e., 10, 12.5, and 16 kHz. Hearing protectors (earmuffs) were used. The subjective (REAT) and objective methods were also used based on the "acoustic text fixture – ATX" – the artificial head of G.R.A.S. 45CB. The authors of this study examined a total of 27 hearing protectors (different companies and types) and obtained large differences in attenuation between individual types of protectors, reaching up to 40 dB at 16 kHz. In addition, they found differences between the attenuation results based on different methods. For the 10 kHz frequency, the average attenuation values determined by the objective method were higher by 6 dB, while for the 12.5 and 16 kHz frequencies they were greater and these differences on average even amounted to 15 dB.

The use of an objective method of measuring the effectiveness of the attenuation obtained by hearing protectors may be particularly useful when it is necessary to assess the degree of exposure to a particularly dangerous impulse (Młyński *et al.*, 2014). Młyński *et al.* (2014) studied the effectiveness of attenuation of two types of hearing protectors (foam earplug and earmuff) in the case of an impulse noise, namely, the impact of a steel hammer at the workplace. In their research they used the objective AFT method. The test results have shown that the highest attenuation efficiency was demonstrated by earplugs.

5. Conclusions

To sum up, the most important conclusions resulting from this work are as follows:

- The results of this study did not confirm the hypothesis that the measurement method had no significant effect on the attenuation characteristics of self-designed custom moulded earplugs with different types of acoustic filters.
- In the case of an objective method of measuring the sound attenuation provided by earplugs, it was shown that in addition to the significant effect of frequency $\{F(6) = 4720.91,\ p < 0.001\}$, the attenuation values also significantly depended on the type of acoustic filter used $\{F(3) = 4225.49,\ p < 0.001\}$.
- The objective measurement method showed that different levels of stimulation (85, 90, and 95 dB) of the test signal, which was pink noise, did not significantly affect the attenuation efficiency for either the full earplug and for the earplugs with F1, F2, and F3 filters.
- Tukey's test showed that at the confidence level of $p = 0.05$, the average attenuation values for earplugs with F3 filters and full earplugs (FE) obtained from objective measurements differ significantly from each other. No statistically significant differences were found in the average attenuation values between earplugs with F1 and F2 filters. It

means that changing the inside diameter of the filter from 1.25 mm to 0.85 mm did not significantly affect the attenuation characteristics.

- The results of the objective method indicated that in the whole frequency range the highest attenuation is shown by the full earplugs, achieving 8 kHz average attenuation slightly above 45 dB. In turn, in the case of earplugs with filters, the maximum attenuation falls in the 2–4 kHz frequency band, and for 4–8 kHz it decreases by about 6 dB.
- The attenuation values obtained from subjective measurements also confirmed that both the frequency $\{F(6) = 111.41,\ p = 0.001\}$ and the type of filter $\{F(3) = 427.77,\ p = 0.001\}$ significantly affect the attenuation values of the tested hearing protectors.
- Just as with the use of the objective measurement method, the subjective method did not indicate significant differences in attenuation when using the F1 and F2 filters.
- The comparison of the average attenuation values of the earplugs over all frequencies and over all types of earplugs with the average attenuation values obtained from the objective and subjective methods showed that overall the measurement method does not significantly affect the mean attenuation values $\{F(1) = 0.36,\ p = 0.547\}$. However, Tukey's post hoc analysis showed that for individual frequencies, the average sound attenuation values (taking into account all types of earplugs) differ significantly for the frequencies of 0.25 kHz and 4 kHz. It means that the mean sound attenuation characteristics determined by two methods differ significantly.

It should be added that the increasingly enhanced systems of artificial ear/artificial head, especially those in which the full projection of the ear canal has been used, gives reason to hope that in the future fully objective measurement of the attenuation provided by any hearing protectors and earplugs will be possible. The research results included in this work are preliminary studies. However, it should be stressed upon that the Head and Torso Simulator Brüel & Kjær Type 5128 does not take into account bone transmission (vibrations), which occurs with the perception of sounds in the auditory system. There is therefore some concern that, especially in the low frequency ranges, where bone conduction plays an important role, differences in acoustic attenuation values may arise with the objective and subjective methods. The plan is to use a custom moulded earplugs with a greater variety of acoustic filters in subsequent research and to significantly increase the group of people surveyed with the subjective method. In addition, future research should take into account an important factor, namely, the propagation of acoustic energy through the bone in the real ear and the modelling of this phenomenon in the artificial head and torso system.

Ethics approval and consent to participate

The research was carried out in accordance with the recommendations of conducting scientific and didactic research with the participation of people specified in the Resolution of the Council of the Faculty of Physics of the University of Adam Mickiewicz in Poznan from December 20, 2013. All subjects agreed to participate in the study.

Availability of data and material

Not applicable.

Competing interests

The authors have no conflict of interest, financial or otherwise.

Funding

Not applicable.

Authors' contributions

RG: Contributions to the conception and design of the study, data acquisition, analysis, results interpretation, and writing the manuscript.

AW: Contributions to the conception and design of the study, analysis, results interpretation, and writing the manuscript.

AD: Design and implementation of the earplugs.

MKK: Data acquisition.

KMH: Data acquisition.

Acknowledgments

We would like to thank dr Mikołaj Baranowski for developing and printing acoustic filters for the earplugs and subjects for participating in the studies. We thank the reviewers for helpful comments on an earlier version of this paper.

References

1. ANSI/ASA-S12.42-2010 (2010), *Methods for the measurement of insertion loss of hearing protection devices in continuous or impulsive noise using microphone-in-real-ear or acoustic test fixture procedures*, Acoustical Society of America, http://webstore.ansi.org/RecordDetail.aspx?sku=ANSI%2FASA+S12.42-2010.

2. Berger E.H. (2005), Preferred methods for measuring hearing protector attenuation, [in:] *Inter-Noise, Environmental Noise Control, The 2005 Congress and Exposition on Noise Control Engineering*, 7–10 August, Rio de Janeiro.
3. Biabani A., Aliabadi M., Golmohammadi R., Farhadian M. (2017), Individual fit testing of hearing protection devices based on microphone in real ear, *Safety and Health at Work*, **8**(4): 364–370, doi: 10.1016/j.shaw.2017.03.005.
4. Bockstael A. *et al.* (2011), Speech recognition in noise with active and passive hearing protectors: a comparative study, *The Journal of the Acoustical Society of America*, **129**(6): 3702–3715, doi: 10.1121/1.3575599.
5. Brown A.D., Beemer B.T., Greene N.T., Argo T. IV., Meegan G.D., Tollin D.J. (2015), Effects of active and passive hearing protection devices on sound source localization, speech recognition, and tone detection, *PLOS ONE*, **10**(8): e0136568, doi: 10.1371/journal.pone.0136568.
6. Davis R.R., Murphy W.J., Byrne D.C., Shaw P.B. (2011), Acceptance of a semi-custom hearing protector by manufacturing workers, *Journal of Occupational and Environmental Hygiene*, **8**(12): D125–130, doi: 10.1080/15459624.2011.626262.
7. Directive 2003/10/EC (2003), Directive 2003/10/EC of the European Parliament and of the Council of 6 February 2003 on the minimum health and safety requirements regarding the exposure of workers to the risks arising from physical agents (noise), [in:] *Directive 2003/10/EC*, European Parliament, Council of the European Union.
8. Fackler C.J., Berger E.H., Murphy W.J., Stergar M.E. (2017), Spectral analysis of hearing protector impulsive insertion loss, *International Journal of Audiology*, **56**(Sup1): 13–21, doi: 10.1080/14992027.2016.1257869.
9. Hiselius P., Edvall N., Reimers D. (2015), To measure the impact of hearing protectors on the perception of speech in noise, *International Journal of Audiology*, **54**(Sup1): S3–S8, doi: 10.3109/14992027.2014.973539.
10. Journal of Laws (2014), The Regulation of the Ministry of Labour and Social Policy of 6 June 2014, item 817, on the maximum permissible concentrations and intensities of agents that are hazardous for health at the workplace.
11. Killion M.C. (2012), Factors influencing use of hearing protection by trumpet players, *Trends in Amplification*, **16**(3): 173–178, doi: 10.1177/1084713812468514.
12. Kozłowski E., Młyński R. (2017), Measurement of earmuffs attenuation at high audible frequencies, *Archives of Acoustics*, **42**(2): 249–254, doi: 10.1515/aoa-2017-0027.
13. Lee K., Casali J.G. (2017), Development of an auditory situation awareness test battery for advanced hearing protectors and TCAPS: detection subtest of DRILCOM (detection-recognition/identification-localization-communication), *International Journal of Audiology*, **56**(Sup1): 22–33, doi: 10.1080/14992027.2016.1256505.
14. Lie A. *et al.* (2016), Occupational noise exposure and hearing: a systematic review, *International Archives of Occupational and Environmental Health*, **89**(3): 351–372, doi: 10.1007/s00420-015-1083-5.
15. Młyński R., Kozłowski E., Adamczyk J. (2014), Assessment of impulse noise hazard and the use of hearing protection devices in workplaces where forging hammers are used, *Archives of Acoustics*, **39**(1): 73–79, doi: 10.2478/aoa-2014-0008.
16. Norin J.A., Emanuel D.C., Letowski T.R. (2011), Speech intelligibility and passive, level-dependent earplugs, *Ear and Hearing*, **32**(5): 642–649, doi: 10.1097/AUD.0b013e31821478c8.
17. PN-EN-ISO 4869-2 (2018), *Acoustics. Hearing protectors – Part 2: estimation of effective A-weighted sound pressure levels when hearing protectors are worn*, Polish Committee for Standardization.
18. PN-EN-ISO-4869-3 (2007), *Acoustics. Hearing protectors – Part 3: Measurement of insertion loss of earmuff type protectors using an acoustic test fixture*, Polish Committee for Standardization.
19. PN-EN-ISO-8253-2 (2010), *Acoustics. Audiometric test methods – Part 2: Sound field audiometry with pure-tone and narrow-band test signals*, Polish Committee for Standardization.
20. PN-EN-ISO-9612 (2011), *Acoustics. Determination of occupational noise exposure – Engineering method*, Polish Committee for Standardization.
21. PN-N-01307 (1994), *Permissible noise values in the workplace. Measurement requirements*, Polish Committee for Standardization.
22. Samelli A.G., Gomes R.F., Chammas T.V., Silva B.G., Moreira R.R., Fiorini A.C. (2018), The Study of Attenuation Levels and the Comfort of Earplugs, *Noise and Health*, **20**(94): 112–119.
23. Śliwińska-Kowalska M., Zaborowski K. (2017), WHO environmental noise guidelines for the european region: a systematic review on environmental noise and permanent hearing loss and tinnitus, *International Journal of Environmental Research and Public Health*, **14**(10): 1–19, doi: 10.3390/ijerph14101139.
24. Zimpfer V., Sarafian D. (2014), Impact of hearing protection devices on sound localization performance, *Frontiers in Neuroscience*, **8**: 1–10, doi: 10.3389/fnins.2014.00135.

Archives of Acoustics Vol. 47, No. 2, pp. 213–221 (2022), doi: 10.24425/aoa.2022.141651

Research Paper

A Honeycomb Based Graded Metamaterial Muffler with Broadband Sound Attenuation and Load Bearing Performances

Gen LI[(1),(2)], Yan CHEN[(1),(2)], Huan HE[(1),(2),(3),(4)]*

[(1)] *State Key Laboratory of Mechanics and Control of Mechanical Structures*
Nanjing University of Aeronautics and Astronautics
Nanjing 210016, China

[(2)] *Institute of Vibration Engineering Research*
Nanjing University of Aeronautics and Astronautics
Nanjing 210016, China

[(3)] *MIIT Key Laboratory of Multi-Functional Lightweight Materials and Structures*
Nanjing 210016, China

[(4)] *Laboratory of Aerospace Entry, Descent and Landing Technology*
Beijing 100094, China
*Corresponding Author e-mail: hehuan@nuaa.edu.cn

(*received November 19, 2021; accepted March 12, 2022*)

A challenge for developing acoustic metamaterials (AMMs) is considering the application of broadband muffling and load bearing capacity simultaneously. In this paper, a honeycomb based graded AMM muffler is proposed, which can widen the attenuation band and improve the structural stiffness without any external device by means of integrated design. Firstly, the acoustic and mechanical characteristics of the muffler unit cell are theoretically and numerically studied, and the graded muffler is designed based on these characteristics. The numerical results show that the graded muffler widens the attenuation bandwidth of the unit cell, and the simulation also shows that the graded muffler has greater stiffness than the uniform one. The stiffness driven muffler provides new possibilities for the design of advanced metamaterial with simultaneous sound insulation and load bearing performances.

Keywords: acoustic metamaterials; honeycomb structure; phononic crystal; local resonance.

1. Introduction

In recent years, phononic crystals (PCs) or acoustic metamaterials (AMMs) have attracted extensive attention due to their unusual ability to manipulate elastic waves and flexible design (Deymier, 2013). By introducing the concept of phonon band gap (Narayanamurti *et al.*, 1979; Sigalas, Economou, 1992; Kushwaha *et al.*, 1993), the sound insulation effect of AMMs can be explained from the perspective of wave mechanics. Band gaps represent frequency ranges where waves cannot pass through. Initially, the generation of band gaps is thought to be attributed to the destructive interference in a periodic structure (Martínez-Sala *et al.*, 1995; Montero de Espinosa *et al.*, 1998; Vasseur *et al.*, 1998; Shao *et al.*, 2020; Chen *et al.*, 2021a; 2021b), so the lattice constant must be of the same scale as the wavelength. Later, due to the low frequency band gaps induced by local resonances (Liu *et al.*, 2000), it is possible for AMMs to control elastic waves by elaborately designed subwavelength scale microstructure (Qian, Shi, 2017), which provides a new solution for low frequency noise reduction. However, the development of AMMs is still restricted by the narrow band gap width and the sensitivity to external load. Many scholars have made impressive contributions to solving these problems by using external devices such as absorbers, circuits, and

magnetic fields (Brennan, 1997; Nishida, Koopmann, 2007; Wang *et al.*, 2011; Popa *et al.*, 2013; Chen *et al.*, 2014; Wang, Chen, 2015; Xiao *et al.*, 2015). In spite of this, it is still challenging to achieve the integrated design of AMMs with broadband sound attenuation and load bearing performances.

Cellular honeycomb structures appear widely in nature and are manufactured on a large scale (Wang, 2019). In the past two decades, a large number of studies has been conducted on the basic mechanical behaviour of honeycomb structures (Camata, Shing, 2010; Asprone *et al.*, 2013; Sun *et al.*, 2017; Li *et al.*, 2018). When honeycomb structures are subjected to out-of-plane compression loads, their stiffness is almost the same as that of solid materials with the same thickness (Fan *et al.*, 2006; Khan *et al.*, 2012). To satisfy the various requirements with the development of scientific engineering, many creative honeycomb based structures are proposed (Michailidis *et al.*, 2009; Correa *et al.*, 2015; Chen *et al.*, 2016; Han *et al.*, 2016; Huang *et al.*, 2016; Wang *et al.*, 2021). By embedding the honeycomb cells with different materials or structures, such as foam, tubes, or even other polymer materials, honeycombs can be designed to have desirable properties (Zarei Mahmoudabadi, Sadighi, 2011; Xiang, Du, 2017; Liu *et al.*, 2018; Wang, Liu, 2018, 2019).

Functionally graded materials (FGMs) are advanced engineering materials designed for a specific performance or function in which a spatial gradation in structure and/or composition lend themselves to tailored properties (Naebe, Shirvanimoghaddam, 2016). Originally, FGMs are designed to relax the internal thermal stress by gradually changing their composition from metallic to ceramic (Kawasaki, Watanabe, 1997). Nowadays, FGMs have extended their applications to electronics, chemistry, optic, biomedicine, nuclear engineering, civil engineering, and many other fields (Koizumi, 1997). A large number of studies has been conducted on the special properties of FGMs (Aboudi *et al.*, 1999; Cheng, 2001; Shen, 2002; Chen, Lee, 2003; Tsukamoto, 2003; Jabbari, Sohrabpour, 2014). In brief, the superior performances of FGMs come from the spatially inhomogeneous composition or microstructure.

In this paper, a honeycomb based graded metamaterial muffler is proposed. By embedding the honeycomb cells with local resonance microstructures, the requirements of noise reduction and bearing capacity can be simultaneously satisfied. As a kind of stiffness driven honeycomb structure, it can be designed to meet the deformation requirements. Acoustically, the honeycomb frame can satisfy the general broadband sound insulation, while the local resonance microstructures are used to attenuate the strong noise in the specific frequency band. The band gap broadening can be realised by the combination of multiple unit cells with lattice constant graded variation. First, we study the muffler unit cell (Fig. 1a) and obtain the relationship between lattice constant and its acoustic and mechanical properties. Then we combine unit cells of different sizes into a graded muffler (Fig. 1b) to widen the band gap. The out-of-plane load bearing capacity of different configurations is also tested numerically. The results show that both the acoustic and mechanical properties of the graded muffler are better than those of the uniform one. Different from conventional acoustic metamaterial, due to the structural and functional integration design, this muffler does not require an external device to adjust the band gap, which means that it has higher reliability and robustness. Compared with membrane type or traditional plate type AMMs, this honeycomb based muffler is more resistant to out-of-plane deformation. In contrast to AMMs relying on soft materials such as rubber, the acoustic band gap of this muffler is independent of the structural material, so different materials can be selected according to the amplitude of the load. Since it is made of single material, it can be conveniently fabricated by additive manufacturing technology, leading to a broad application prospect. For instance, periodic graded mufflers (Fig. 1c) can be used as a sound insulation floor of an aircraft cabin (Fig. 1d) thus providing a quieter environment for passengers.

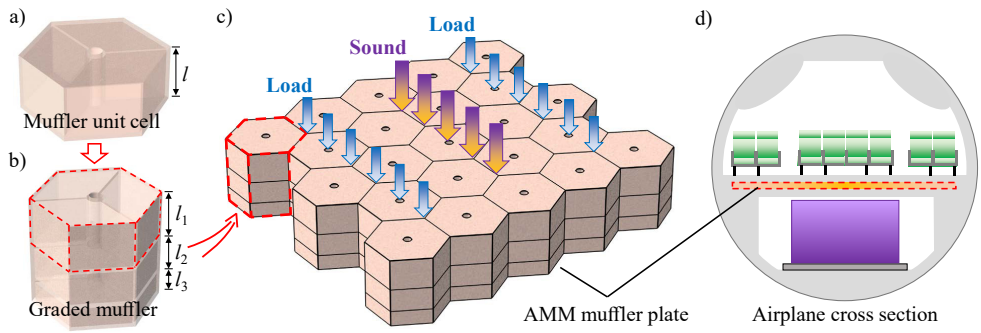

Fig. 1. Honeycomb based graded metamaterial muffler: a) the muffler unit cell of lattice constant l; b) a graded muffler consisting of three unit cells with different lattice constants; c) an AMM muffler plate consisting of multiple graded mufflers arranged periodically; d) potential application in aircraft.

2. Theoretical model of unit cell

As shown in Fig. 2, the unit cell can be considered to be composed of three reinforcing ribs and a perforated cylindrical tube on the basis of a honeycomb cell. The geometric parameters of one unit cell are represented schematically by the explosion view and cross section. Here, l represents the lattice constant, a represents the side length of the regular hexagon, r_1 is the tube inner radius, r_2 is the perforation radius, t represents the honeycomb cell-wall thickness, tube wall thickness, reinforcing rib thickness, and end cover thickness. In this paper, the acoustic impedance of all possible solid materials is much higher than that of air, so from the perspective of aeroacoustics, all solid material boundaries can be regarded as hard acoustic field boundaries.

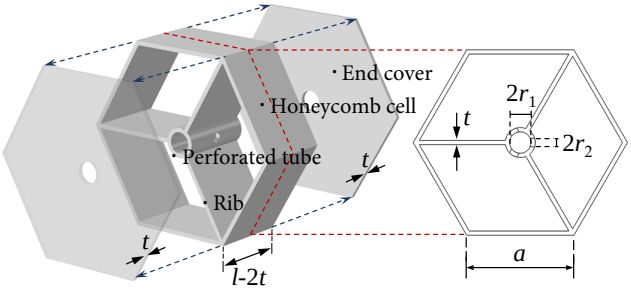

Fig. 2. Schematic illustration of the muffler unit cell with geometric parameters.

The unit cell contains three cavities, each of which works as an acoustic chamber resembling a Helmholtz resonator. When the resonator vibrates, it will radiate sound field to the surrounding medium, and the resonator will be affected by the field generated by itself. Consider a piston acoustic source of radius r_2 that vibrates at velocity $u = \overline{u}\exp(j\omega t)$, where $j = \sqrt{-1}$ is imaginary unit, ω is angular frequency, The additional radiation impedance (Junger, Feit, 1986) is given by:

$$Z_r = \rho_a c_a \pi r_2^2 \left[1 - \frac{J_1(2kr_2)}{kr_2} + j\frac{K_1(2kr_2)}{2(kr_2)^2}\right], \tag{1}$$

where J_1 is the Bessel function of first kind for order one, K_1 is the modified Bessel function of second kind for order one, k is wavenumber, ρ_a and c_a are the density and sound speed of air. When $kr_2 < 1$, the piston radiation reactance X_r can be obtained from the imaginary part of Z_r, that is, $X_r = \mathrm{Im}(Z_r) \approx 8\rho_a c_a k r_2^3/3$. Considering that the oscillator radiates in both positive and negative directions, the additional mass can be obtained as

$$M_r = \frac{2X_r}{\omega} = \frac{16}{3}\rho_a r_2^3. \tag{2}$$

Thus, the resonant frequency of Helmholtz resonator considering the additional mass correction caused by acoustic radiation can be written as:

$$f_H = \sqrt{\frac{\pi(r_2 c_a)^2}{4\pi^2 V_H\left[t + M_r/(\rho_a \pi r_2^2)\right]}}, \tag{3}$$

where

$$\begin{aligned} V_H &= (a^2/2 - \pi r_1^2/3)(l - 2t) \\ &\quad - \left(\sqrt{3}a - r_1 + 2\pi r_1/3\right)(l - 2t)t \\ &\quad + \left(1/2 - \sqrt{3}/6 - \pi/3\right)(l - 2t)t^2 \end{aligned}$$

is the acoustic chamber volume. To filter out acoustic waves at undesired frequencies, called target frequencies here, the design parameters should be adjusted so that the Helmholtz resonance frequency is equal to the target frequency.

Then consider the out-of-plane mechanics properties of the unit cell. Here the function of the honeycomb based unit cell is carrying normal loads in planes containing the axis of the hexagonal prism. The compressive moduli of the cell walls or ribs are much larger than the flexural moduli of the end covers. Thus, it is assumed that the carrying capacity of the end cover can be ignored. In addition, it is necessary to consider the negative effect of perforations on the bearing capacity of the cylindrical tube. An equivalent section method is adopted to simplify the part of the tube wall with a perforation to a wall of constant thickness, as shown in Fig. 3. The volume of the tube remains constant before and after the simplification, by which we can obtain the equivalent thickness

$$t_{eq} = \left[1 - \frac{2r_1 r_2^2}{l(2r_1 + t)\sqrt{r_1^2 - r_2^2}}\right]t, \tag{4}$$

and the equivalent cross sectional area of the unit cell

$$\begin{aligned} A_{eq} &= 3\pi(r_1 + t/2)\,t_{eq} + (9a - 3r_1 - \pi r_1)\,t \\ &\quad - \left(4\sqrt{3} + 3 + \pi/2\right)t^2. \end{aligned} \tag{5}$$

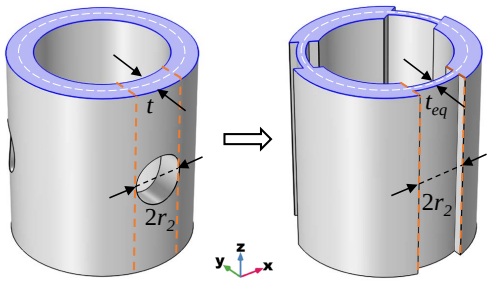

Fig. 3. Equivalent simplification of the perforated cylindrical tube.

It should be noted that the compressional wave velocity of the solid material c_s is equal to that of the unit cell c^*, that is

$$\sqrt{E_s/\rho_s} = \sqrt{E_c^*/\rho^*}, \tag{6}$$

where E_s and ρ_s are the Young's modulus and density of the solid material, respectively, E_c^* is the compressive modulus of the unit cell, and $\rho^* = m/(A^* l)$ is the density of the unit cell with $A^* = 3\sqrt{3}a^2/2$ being the area of the regular hexagon and m being the mass of the unit cell. Throughout, the subscript s refers to a property of the solid material while a superscripted * indicates an equivalent property of the unit cell itself. Accordingly, the compressive modulus of the unit cell is given by

$$E_c^* = \frac{E_s A_{eq}}{A^*}. \tag{7}$$

3. Finite element model

The range of acoustic band gap can be determined by the phonon dispersion curves, which, however, cannot reflect the attenuation degree of acoustic waves. Acoustic transmission loss (TL) can be used to demonstrate the effect of structure on acoustic wave attenuation at different frequencies. Phonon dispersion analysis and acoustic TL analysis can be conveniently introduced by taking the air domain inside the muffler structure as a unit cell either, here called an air unit cell to distinguish it from the original muffler unit cell. We assume small deformations here, and therefore neglect acoustoelastic coupling. FE models of the air unit cell (Fig. 4a) and muffler unit cell (Fig. 4b) are established to reveal acoustic and mechanical properties of unit cells with different lattice constants l through COMSOL Multiphysics. Bloch periodic boundary conditions (Bloch, 1929) are set on the two highlighted end faces in Fig. 4a for phonon dispersion analysis. When TL analysis is needed, the plane wave radiation boundary condition is set on one of the highlighted faces in Fig. 4a, and the perfect matching layer is set on the other face. Acoustic TL is defined as $\mathrm{TL} = 10\log(I_i/I_t)$, where I_i and I_t are the sound intensity of the incident wave and transmitted wave, respectively. To obtain the compression stiffness k^* and specific modulus E_c^*/ρ^* of the unit cell, a displacement w in the negative direction of z-axis is applied to the highlighted surface in Fig. 4b, and the z-axis displacement of the bottom surface is set to zero. The stiffness is calculated by $k^* = -f_c/w$. Then from the axial stress-strain relationship we can obtain the specific modulus $E_c^*/\rho^* = -f_c l/(\rho^* A^* w)$, where f_c is the constraining force on the bottom surface.

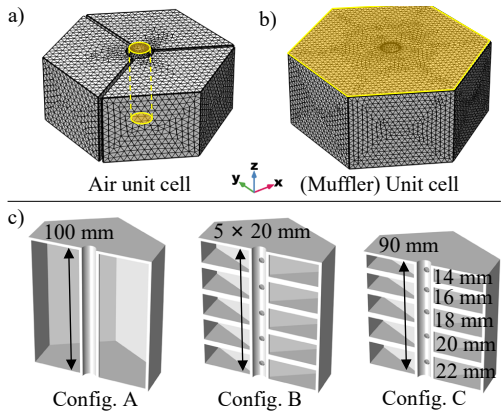

Fig. 4. a) Finite element model for the air domain (or air unit cell) enclosed by the muffler; b) a finite element model for the muffler unit cell; c) three different configurations of a honeycomb based muffler.

Three different configurations are designed to verify the performances of the honeycomb based unit cell and the superiority of graded muffler structure as shown in Fig. 4c. Configuration A is a common honeycomb cell with the reinforcing tube. Configuration B consists of five identical unit cells with the lattice constant of 20 mm. Configuration C is a graded metamaterial muffler with the total length of 90 mm, composed of five unit cells with graded changes in lattice constants. FE method (COMSOL Multiphysics) is used to calculate the TL and linear compression stiffness of the three configurations to compare their acoustic and mechanical properties.

4. Results and discussions

In this section, we first study the acoustic and mechanical properties of the muffler unit cell and then explore the influence of graded combination mode, namely, the offset ratio, on the performance of the muffler. Considering that the lattice constant corresponding to the target frequency is l, the offset ratio is defined as $\alpha = \Delta l/l$, where Δl is the deviation from the central lattice constant. Based on these studies, a graded muffler is designed and manufactured, and its sound insulation performance is tested by numerical methods. The improvement of sound insulation performance can be verified by comparing it with the other two configurations. In the following theoretical and numerical calculations, the physical parameters of air include: the density $\rho_a = 1.2\ \mathrm{kg/m^3}$, sound speed $c_a = 343.2\ \mathrm{m/s}$, dynamic viscosity $\eta_a = 1.84{\cdot}10^{-5}\ \mathrm{Pa\cdot s}$, bulk viscosity $\eta_B = 1.09\cdot 10^{-5}\ \mathrm{Pa\cdot s}$, ratio of specific heat $\gamma_a = 1.4$, specific heat capacity $C_a = 1000\ \mathrm{J/(kg\cdot K)}$, and thermal conductivity $\kappa_a = 0.026\ \mathrm{W/(m\cdot K)}$. The physical parameters of the solid material in the theoretical and numerical calculations include: the density $\rho_s = 2600\ \mathrm{kg/m^3}$, Young's modulus $E_s = 70$ GPa, and Poisson's ratio $\nu_s = 0.3$. As shown in Fig. 2, the geometric parameters of the unit cell include: the regular hexagon side length $a = 50$ mm, the cylindrical tube inner radius $r_1 = 5$ mm and perforation radius $r_2 = 2$ mm, the thickness $t = 2$ mm.

4.1. Acoustic band gap of the unit cell

As shown in Fig. 5a, the acoustic band gap of the unit cell is given by the upper and lower edges, the

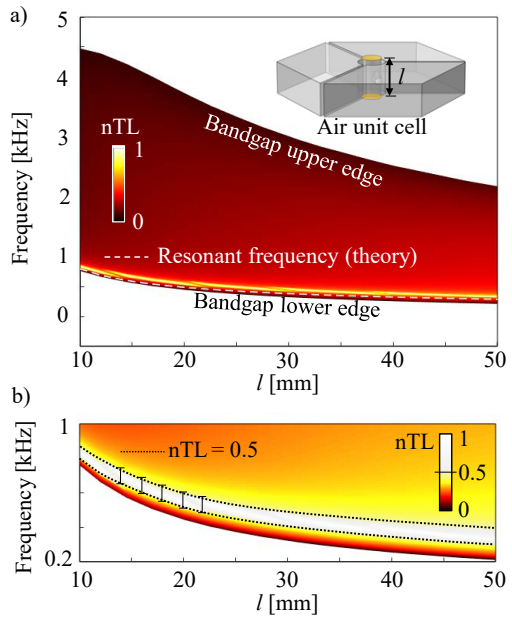

Fig. 5. a) Influences of the lattice constant on acoustic band gap frequency range and normalised transmission loss; b) a partial enlarged drawing of Fig. 5a.

detailed sound insulation capability at different frequencies within the band gap is denoted by the colour legend, and the white dashed line represents the Helmholtz resonance frequencies for different lattice constants calculated by theoretical model. Here, the normalised TL (nTL) is adopted because we are mainly concerned with the variation pattern of the peak frequency of sound insulation with respect to the lattice constant, rather than the absolute sound insulation. The maximum value of TL is set to 1 and the minimum value is set to 0. Overall, the theoretical and finite element model match well. It can be observed from Fig. 5a that the band gap beginning frequency is closely followed by the resonant frequency or target frequency. The unit cell has a wide acoustic band gap, but the nTL is not uniformly distributed in the band gap range. The sound insulation is significantly effective near the resonant frequency, as the incident wave frequency moves away from the resonant point, the normalised TL decreases sharply, as shown in Fig. 5b. These phenomena result from the local resonance mechanism (Liu *et al.*, 2005; Ding *et al.*, 2007; Zhou *et al.*, 2017), which can realise wave control by subwavelength structure but often leads to a strong but narrow attenuation band. As shown in Fig. 5b, compared with the gap bandwidth obtained by the dispersion curves, the actual sound insulation bandwidth considered to be effective ($\mathrm{nTL} \geq 0.5$) is very narrow. We can use the band gap range with strong sound insulation effect ($\mathrm{nTL} \geq 0.5$) to control the strong sound source of specific frequency, while the other band gap range is used for general frequency band insulation. Therefore, we consider combining unit cells with different lattice constants to form a graded structure for broadband sound attenuation. The band gap of $\mathrm{nTL} \geq 0.5$ is used as the design basis. It is noted that when the lattice constant l is smaller than 25 mm, the band gap frequency is more sensitive to the variation of the lattice constant.

4.2. Load bearing capability of the unit cell

The mechanical properties of unit cells with different lattice constants are shown in Fig. 6. The theory and the numerical results agree very well. The mechanical properties are described from two perspectives. The specific compression modulus (or specific modulus) characterises the equivalent properties of a muffler unit cell as a material, while the compression stiffness more directly reflects the ability of the unit cell as a structure to resist deformation. As the lattice constant increases, the specific modulus goes up, but the stiffness decreases, indicating an increase in relative efficiency against physical deformation, but a decrease in absolute resistance to deformation. Hence, the lattice constants should be selected according to practical needs in engineering applications.

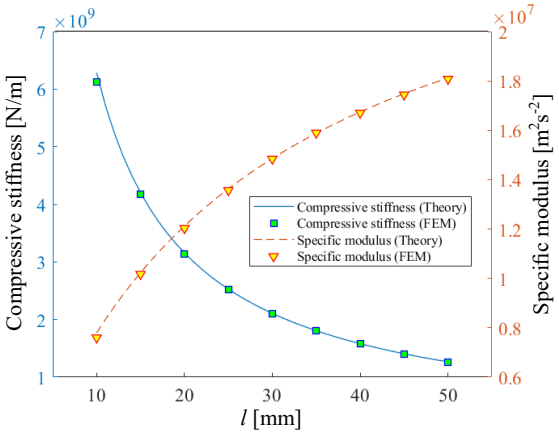

Fig. 6. Influences of the lattice constant on the unit cell compressive stiffness and specific modulus.

4.3. Influence of offset ratio

The influences of offset ratio α on the transmission loss and stiffness of graded structure are shown in Fig. 7. Considering that the lattice constant corresponding to the target frequency is l, the offset ratio is defined as $\alpha = \Delta l/l$, where Δl is the deviation from the central lattice constant. Here, a five-unit-cell graded structure is used to investigate the influence of offset ratio. The lattice constants of these five cells are $(1-2\alpha)l$, $(1-\alpha)l$, l, $(1+\alpha)l$, and $(1+2\alpha)l$. For $l = 20$ mm, the influence of the offset ratio on sound insulation is shown in Fig. 7a. It can be seen that as the offset ratio increases, the effective band gap width

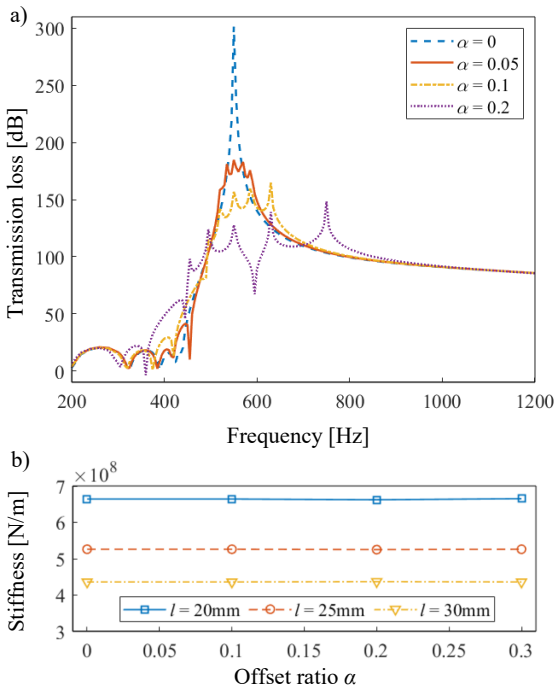

Fig. 7. Influence of the offset ratio on: a) transmission loss; b) compression stiffness under different lattice constants.

(nTL ≥ 0.5) becomes wider, but the attenuation magnitude of the peak transmission loss decreases. When the offset ratio is relatively small, such as 0.05, the peak is barely broadened. When the offset ratio is selected as a relatively large value, such as 0.2, the attenuation peak is divided into five separate parts, which is not expected to happen with band structures. Therefore, in order to achieve a wide and relatively high attenuation band gap, a medium α value, such as 0.1, is acceptable. The influence of the offset ratio on compression stiffness under different lattice constants is shown in Fig. 7b. It can be seen that the stiffness is negatively correlated with the lattice constant, but almost does not change with the offset ratio. This is because the horizontal cover plates are not the main components to bear axial compression, and the position of the covers has negligible effect on the stiffness, which brings more design flexibility.

4.4. Acoustic and mechanical properties of graded mufflers

As a result, five unit cells with lattice constants of 14 mm, 16 mm, 18 mm, 20 mm, and 22 mm are combined to construct a graded composite muffler (configuration C) for band gap broadening. The offset ratio of configuration C is 0.11, which is a moderate value, thus achieving a wide and relatively high attenuation gap. We compare the sound insulation characteristics of ordinary honeycomb cell (configuration A), uniform periodic muffler (configuration B), and graded composite muffler (configuration C), as shown in Fig. 8. Configuration A has no sound insulation peak due to the absence of acoustic chambers. Configuration B has only one sharp TL peak because of its single resonant frequency. Configuration C has five peaks resulting from five different acoustic chambers. Compared with configuration B, configuration C has a smaller TL peak value, but the effective band gap width (nTL ≥ 0.5) is 47% wider, and geometrically configuration C is only 90% the size of configuration B, which means it is lighter and takes up less space. This broadband attenuation effect is numerically confirmed.

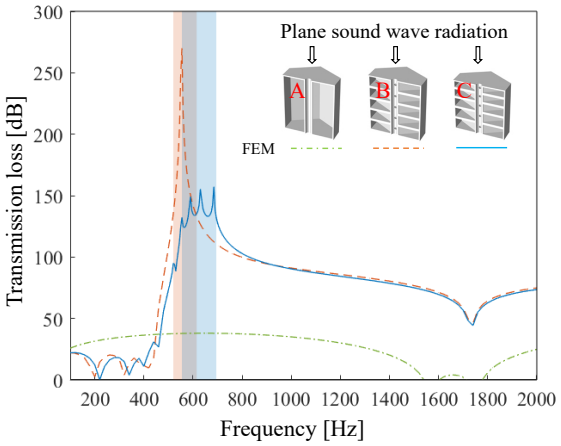

Fig. 8. Transmission loss of the three different muffler configurations.

To investigate the frequency dependent sound pressure distribution of the wave propagation path, its FE volume plots of sound pressure level (SPL) are presented in Fig. 9 at typical frequencies including 555 Hz (the TL peak frequency for both configuration B and configuration C) and 685 Hz (the TL peak frequency only for configuration C). The reference sound pressure is 20 μPa. It can be seen from Fig. 9 that the SPL in configuration B varies uniformly. At its TL peak frequency of 555 Hz (Fig. 9a), SPL drops evenly and rapidly along the sound propagation path. At 685 Hz (Fig. 9b), the SPL decreases relatively slowly, but still varies in a uniform way. For configuration C, when the incident wave frequency is equal to the resonant frequency of one of the acoustic cavities, a rapid drop of SPL occurs near this cavity, and this phenomenon is particularly obvious in Fig. 9d. At the acoustic cavity indicated by the arrow, the SPL drops by about 63 dB. It is the presence of multiple resonant frequencies that allows configuration C to have a broader band gap compared with configuration B, at the expense of part of the single frequency absorption capacity.

Through numerical simulation, the structural compressive stiffness of the three configurations A, B, and C (Fig. 4c) is obtained, which is $K_A = 4.62 \cdot 10^8$ N/m, $K_B = 6.64 \cdot 10^8$ N/m, and $K_C = 7.41 \cdot 10^8$ N/m, respectively. Configuration A (common honeycomb cell)

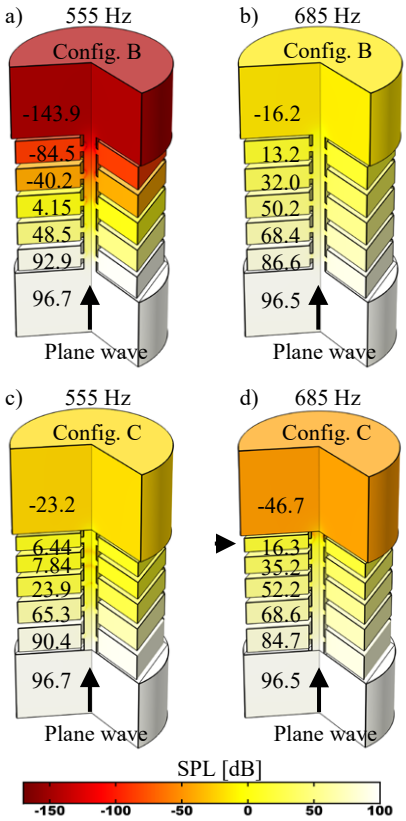

Fig. 9. Sound pressure level distributions of the two configurations of mufflers (configuration B and configuration C) at 555 Hz and 685 Hz.

has the worst stiffness characteristics. Configuration C (graded muffler) has 11.6% higher stiffness than that of configuration B (uniform periodic muffler) while its length is 10% shorter and the mass is 4.5% lighter. This is because shorter and lighter unit cells have greater stiffness, as shown in Fig. 7b. Due to the series arrangement of unit cells in configurations B and C, we can estimate the equivalent stiffness of the two structures by regarding them as multiple springs in series. That is, a single unit cell is regarded as a spring, and a combination of multiple cells is regarded as a series of springs. According to the stiffness of a unit cell obtained in Subsec. 4.2, $K_B = 6.31 \cdot 10^8$ N/m and $K_C = 7.12 \cdot 10^8$ N/m are calculated by the spring series formula, neither deviation from the numerical result is more than 5%.

5. Conclusion

The proposed honeycomb based graded metamaterial muffler shows excellent broadband sound attenuation and stiffness properties. Based on the Helmholtz resonance theory and cellular solids theory, acoustic and mechanical theoretical models are established, respectively. Also, different finite element models are developed via the commercial software COMSOL Multiphysics for comparison. The finite element calculation results match well with the theoretical results. The results show that acoustic metamaterials can be used as both structural and functional materials by setting up resonance structures in cellular solids. In addition, by introducing graded structure design, the effective subwavelength band gap can be extended at a certain offset ratio, at the cost of the loss of acceptable single frequency muffling effect. The graded muffler is superior to the uniform muffler in the noise elimination effect and stiffness characteristics. Therefore, the proposed metamaterial muffler achieves broadband sound attenuation without loss of bearing performance, which shows promising potential for noise control engineering.

Acknowledgments

The presented work is funded by National Natural Science Foundation of China (Grant No. 12072153).

References

1. Aboudi J., Pindera M.-J., Arnold S.M. (1999), Higher-order theory for functionally graded materials, *Composites Part B: Engineering*, **30**(8): 777–832, doi: 10.1016/S1359-8368(99)00053-0.

2. Asprone D., Auricchio F., Menna C., Morganti S., Prota A., Reali A. (2013), Statistical finite element analysis of the buckling behavior of honeycomb structures, *Composite Structures*, **105**: 240–255, doi: 10.1016/j.compstruct.2013.05.014.

3. Bloch F. (1929), About the quantum mechanics of electrons in crystal lattices [in German], *Zeitschrift für Physik*, **52**(7): 555–600, doi: 10.1007/BF01339455.

4. Brennan M.J. (1997), Characteristics of a wideband vibration neutralizer, *Noise Control Engineering Journal*, **45**(5): 201–207, doi: 10.3397/1.2828441.

5. Camata G., Shing P.B. (2010), Static and fatigue load performance of a GFRP honeycomb bridge deck, *Composites Part B: Engineering*, **41**(4): 299–307, doi: 10.1016/j.compositesb.2010.02.005.

6. Chen Q. *et al.* (2016), Plastic collapse of cylindrical shell-plate periodic honeycombs under uniaxial compression: experimental and numerical analyses, *International Journal of Mechanical Sciences*, **111–112**: 125–133, doi: 10.1016/j.ijmecsci.2016.03.020.

7. Chen W.Q., Lee K.Y. (2003), Alternative state space formulations for magnetoelectric thermoelasticity with transverse isotropy and the application to bending analysis of nonhomogeneous plates, *International Journal of Solids and Structures*, **40**(21): 5689–5705, doi: 10.1016/S0020-7683(03)00339-1.

8. Chen X., Xu X., Ai S., Chen H., Pei Y., Zhou X. (2014), Active acoustic metamaterials with tunable effective mass density by gradient magnetic fields, *Applied Physics Letters*, **105**(7): 071913, doi: 10.1063/1.4893921.

9. Chen Y., Chen G., Li G., He H. (2021a), Modal analysis of flexural band gaps in a membrane acoustic metamaterial (MAM) and waveguides affected by shape characteristics, *Physics Letters A*, **414**: 127635, doi: 10.1016/j.physleta.2021.127635.
10. Chen Y., Li G., Sun R., Chen G. (2021b), Wave dispersion in one-dimensional nonlinear local resonance phononic crystals with perturbation method, *Crystals*, **11**(7): 1–15, doi: 10.3390/cryst11070774.
11. Cheng Z.-Q. (2001), Nonlinear bending of inhomogeneous plates, *Engineering Structures*, **23**(10): 1359–1363, doi: 10.1016/S0141-0296(01)00017-7.
12. Correa D.M., Seepersad C.C., Haberman M.R. (2015), Mechanical design of negative stiffness honeycomb materials, *Integrating Materials and Manufacturing Innovation*, **4**(1): 165–175, doi: 10.1186/s40192-015-0038-8.
13. Deymier P.A. [Ed.] (2013), *Acoustic Metamaterials and Phononic Crystals*, Springer, doi: 10.1007/978-3-642-31232-8.
14. Ding Y., Liu Z., Qiu C., Shi J. (2007), Metamaterial with simultaneously negative bulk modulus and mass density, *Physical Review Letters*, **99**(9): 2–5, doi: 10.1103/PhysRevLett.99.093904.
15. Fan X., Verpoest I., Vandepitte D. (2006), Finite element analysis of out-of-plane compressive properties of thermoplastic honeycomb, *Journal of Sandwich Structures & Materials*, **8**(5): 437–458, doi: 10.1177/1099636206065862.
16. Han B., Wang W., Zhang Z., Zhang Q., Jin F., Lu T. (2016), Performance enhancement of sandwich panels with honeycomb–corrugation hybrid core, *Theoretical and Applied Mechanics Letters*, **6**(1): 54–59, doi: 10.1016/j.taml.2016.01.001.
17. Huang J., Gong X., Zhang Q., Scarpa F., Liu Y., Leng J. (2016), In-plane mechanics of a novel zero Poisson's ratio honeycomb core, *Composites Part B: Engineering*, **89**: 67–76, doi: 10.1016/j.compositesb.2015.11.032.
18. Jabbari M., Sohrabpour S. (2014), Mechanical and thermal stresses in a functionally graded hollow cylinder due to nonaxisymmetric steady-state loads, [in:] *Encyclopedia of Thermal Stresses,* Hetnarski R.B. [Ed.], pp. 2946–2952, Springer, Dordrecht, doi: 10.1007/978-94-007-2739-7_959.
19. Junger M.C., Feit D. (1986), *Sound, structures, and their interaction*, The MIT Press: Cambridge, Massachusetts, London, England.
20. Kawasaki A., Watanabe R. (1997), Concept and P/M fabrication of functionally gradient materials, *Ceramics International*, **23**(1): 73–83, doi: 10.1016/0272-8842(95)00143-3.
21. Khan M.K., Baig T., Mirza S. (2012), Experimental investigation of in-plane and out-of-plane crushing of aluminum honeycomb, *Materials Science and Engineering: A*, **539**: 135–142, doi: 10.1016/j.msea.2012.01.070.
22. Koizumi M. (1997), FGM activities in Japan, *Composites Part B: Engineering*, **28**(1–2): 1–4, doi: 10.1016/S1359-8368(96)00016-9.
23. Kushwaha M.S., Halevi P., Dobrzynski L., Djafari-Rouhani B. (1993), Acoustic band structure of periodic elastic composites, *Physical Review Letters*, **71**(13): 2022–2025, doi: 10.1103/PhysRevB.49.2313.
24. Li Z., Wang T., Jiang Y., Wang L., Liu D. (2018), Design-oriented crushing analysis of hexagonal honeycomb core under in-plane compression, *Composite Structures*, **187**: 429–438, doi: 10.1016/j.compstruct.2017.12.066.
25. Liu J., Wang Z., Hui D. (2018), Blast resistance and parametric study of sandwich structure consisting of honeycomb core filled with circular metallic tubes, *Composites Part B: Engineering*, **145**: 261–269, doi: 10.1016/j.compositesb.2018.03.005.
26. Liu Z. *et al.* (2000), Locally resonant sonic materials, *Science*, **289**(5485): 1734–1736, doi: 10.1126/science.289.5485.1734.
27. Liu Z., Chan C.T., Sheng P. (2005), Analytic model of phononic crystals with local resonances, *Physical Review B – Condensed Matter and Materials Physics*, **71**(1): 1–8, doi: 10.1103/PhysRevB.71.014103.
28. Martínez-Sala R., Sancho J., Sánchez J.V., Gómez V., Llinares J., Meseguer F. (1995), Sound attenuation by sculpture, *Nature*, **378**(6554): 241, doi: 10.1038/378241a0.
29. Michailidis P.A., Triantafyllidis N., Shaw J.A., Grummon D.S. (2009), Superelasticity and stability of a shape memory alloy hexagonal honeycomb under in-plane compression, *International Journal of Solids and Structures*, **46**(13): 2724–2738, doi: 10.1016/j.ijsolstr.2009.03.013.
30. Montero de Espinosa F.R., Jiménez E., Torres M. (1998), Ultrasonic Band Gap in a Periodic Two-Dimensional Composite, *Physical Review Letters*, **80**(6–9): 1208–1211, doi: 10.1103/PhysRevLett.80.1208.
31. Naebe M., Shirvanimoghaddam K. (2016), Functionally graded materials: A review of fabrication and properties, *Applied Materials Today*, **5**: 223–245, doi: 10.1016/j.apmt.2016.10.001.
32. Narayanamurti V., Strömer H.L., Chin M.A., Gossard A.C., Wiegmann W. (1979), Selective transmission of high-frequency phonons by a superlattice: the "dielectric" phonon filter, *Physical Review Letters*, **43**(27): 2012–2016, doi: 10.1103/PhysRevLett.43.2012.
33. Nishida E., Koopmann G.H. (2007), A method for designing and fabricating broadband vibration absorbers for structural noise control, *Journal of Vibration and Acoustics, Transactions of the ASME*, **129**(4): 397–405, doi: 10.1115/1.2424968.
34. Popa B.I., Zigoneanu L., Cummer S.A. (2013), Tunable active acoustic metamaterials, *Physical Review B – Condensed Matter and Materials Physics*, **88**(2): 1–8, doi: 10.1103/PhysRevB.88.024303.

35. Qian D., Shi Z. (2017), Using PWE/FE method to calculate the band structures of the semi-infinite PCs: periodic in x-y plane and finite in z–direction, *Archives of Acoustics*, **42**(4): 735–742, doi: 10.1515/aoa-2017-0076.

36. Shao H., He H., Chen G., Chen Y. (2020), Two new designs of lamp-type piezoelectric metamaterials for active wave propagation control, *Chinese Journal of Physics*, **65**: 1–13, doi: 10.1016/j.cjph.2020.02.015.

37. Shen H.-S. (2002), Postbuckling analysis of axially loaded functionally graded cylindrical panels in thermal environments, *International Journal of Solids and Structures*, **39**(24): 5991–6010, doi: 10.1016/S0020-7683(02)00479-1.

38. Sigalas M.M., Economou E.N. (1992), Elastic and acoustic wave band structure, *Journal of Sound and Vibration*, **158**(2): 377–382, doi: 10.1016/0022-460X(92)90059-7.

39. Sun G., Hou X., Chen D., Li Q. (2017), Experimental and numerical study on honeycomb sandwich panels under bending and in-panel compression, *Materials & Design*, **133**: 154–168, doi: 10.1016/j.matdes.2017.07.057.

40. Tsukamoto H. (2003), Analytical method of inelastic thermal stresses in a functionally graded material plate by a combination of micro- and macromechanical approaches, *Composites Part B: Engineering*, **34**(6): 561–568, doi: 10.1016/S1359-8368(02)00037-9.

41. Vasseur J.O., Deymier P.A., Frantziskonis G., Hong G., Djafari-Rouhani B., Dobrzynski L. (1998), Experimental evidence for the existence of absolute acoustic band gaps in two-dimensional periodic composite media, *Journal of Physics: Condensed Matter*, **10**(27): 6051–6064, doi: 10.1088/0953-8984/10/27/006.

42. Wang G., Chen S. (2015), Large low-frequency vibration attenuation induced by arrays of piezoelectric patches shunted with amplifier–resonator feedback circuits, *Smart Materials and Structures*, **25**(1): 15004, doi: 10.1088/0964-1726/25/1/015004.

43. Wang G., Wang J., Chen S., Wen J. (2011), Vibration attenuations induced by periodic arrays of piezoelectric patches connected by enhanced resonant shunting circuits, *Smart Materials and Structures*, **20**(12): 125019, doi: 10.1088/0964-1726/20/12/125019.

44. Wang T., An J., He H., Wen X., Xi X. (2021), A novel 3D impact energy absorption structure with negative Poisson's ratio and its application in aircraft crashworthiness, *Composite Structures*, **262**: 113663, doi: 10.1016/j.compstruct.2021.113663.

45. Wang Z. (2019), Recent advances in novel metallic honeycomb structure, *Composites Part B: Engineering*, **166**: 731–741, doi: 10.1016/j.compositesb.2019.02.011.

46. Wang Z., Liu J. (2018), Mechanical performance of honeycomb filled with circular CFRP tubes, *Composites Part B: Engineering*, **135**: 232–241, doi: 10.1016/j.compositesb.2017.09.048.

47. Wang Z., Liu J. (2019), Numerical and theoretical analysis of honeycomb structure filled with circular aluminum tubes subjected to axial compression, *Composites Part B: Engineering*, **165**: 626–635, doi: 10.1016/j.compositesb.2019.01.070.

48. Xiang J., Du J. (2017), Energy absorption characteristics of bio-inspired honeycomb structure under axial impact loading, *Materials Science and Engineering: A*, **696**: 283–289, doi: 10.1016/j.msea.2017.04.044.

49. Xiao S., Ma G., Li Y., Yang Z., Sheng P. (2015), Active control of membrane-type acoustic metamaterial by electric field, *Applied Physics Letters*, **106**(9), doi: 10.1063/1.4913999.

50. Zarei Mahmoudabadi M., Sadighi M. (2011), A study on the static and dynamic loading of the foam filled metal hexagonal honeycomb – Theoretical and experimental, *Materials Science and Engineering: A*, **530**: 333–343, doi: 10.1016/j.msea.2011.09.093.

51. Zhou J., Wang K., Xu D., Ouyang H. (2017), Multi-low-frequency flexural wave attenuation in Euler–Bernoulli beams using local resonators containing negative-stiffness mechanisms, *Physics Letters A*, **381**(37): 3141–3148, doi: 10.1016/j.physleta.2017.08.020.